

MicroRNA-143-3p suppresses cell growth and invasion in laryngeal squamous cell carcinoma via targeting the k-Ras/Raf/MEK/ERK signaling pathway

FENG ZHANG and HUA CAO

Ear Nose and Throat Hospital, The First Affiliated Hospital of Zhengzhou University,
Zhengzhou, Henan 450052, P.R. China

Received November 23, 2017; Accepted July 2, 2018

DOI: 10.3892/ijo.2018.4655

Abstract. MicroRNAs (miRNAs or miRs) have been identified as an important regulator in carcinogenesis and other pathological processes. However, the molecular mechanism underlying the function of miRNAs in the progression and development of laryngeal squamous cell carcinoma (LSCC) remains to be fully elucidated. In the present study, the miRNA expression pattern in LSCC tissues was profiled using miRNA microarray analysis. It was found that a large set of miRNAs are aberrantly expressed in LSCC tissues and that miR-143-3p was the most markedly downregulated compared with normal tissues. The low expression of miR-143-3p was associated with poor prognosis in LSCC. The overexpression of miR-143-3p repressed cellular proliferation and induced apoptosis *in vitro*, and inhibited tumor growth *in vivo*. The upregulation of miR-143-3p suppressed cell migration and invasion through inhibiting the epithelial-mesenchymal transition cascade. In addition, it was verified that the oncogene k-Ras is a target of miR-143-3p in LSCC cells, and the suppressive effects of miR-143-3p on LSCC cells were abrogated by the overexpression of k-Ras. It was also revealed that miR-143-3p may inhibit cell growth and metastasis through targeting the k-Ras/Raf/mitogen-activated protein kinase kinase (MEK)/extracellular signal-regulated kinase (ERK) signaling pathway. Taken together, the data indicated that the miR-143-3p/k-Ras/Raf/MEK/ERK axis serves a key regulator in the development and progression of LSCC, suggesting that miR-143-3p may be a potential prognostic biomarker and therapeutic target in the treatment of LSCC.

Introduction

Head and neck squamous cell carcinoma is considered to be the sixth most common type of cancer worldwide, among which the laryngeal squamous cell carcinoma (LSCC) is a common malignant neoplasm (1). The incidence of LSCC in China has been increasing gradually, particularly in the northeast region (2). Current treatments have a moderate effect in patients with early stage disease, including radiation therapy, chemotherapy and surgical intervention, however, these are less effective for more advanced disease (3). Regional lymph node metastasis and distant metastasis are considered to be the major factors that negatively affect the survival rates of patients with LSCC (4). It is necessary to understand the molecular mechanisms underlying the progression of LSCC in the diagnosis and therapy of LSCC.

MicroRNAs (miRNAs or miRs) are a class of endogenous, non-coding, small, single-stranded RNAs consisting of 18-25 nucleotides, which mediate the post-transcriptional regulation of target genes via inhibiting translation or inducing RNA degradation (5,6). Increasing evidence has demonstrated that miRNAs can function as oncogenes or tumor suppressor genes in cancer, and can suppress cell signaling pathways to modulate various cancer cell processes, including cell proliferation, apoptosis, differentiation and migration (7,8). The ectopic expression of miRNAs is key in the development of LSCC (9), and certain miRNAs directly modulate the apoptosis, proliferation and invasion of LSCC cells (3,10). Tian *et al* revealed that miRNA (miR)-203 is downregulated in LSCC tissues and cells, and that the overexpression of miR-203 represses proliferation and invasion, induces apoptosis and causes cell cycle arrest of Hep-2 cells *in vitro* (10). miR-21 has been identified to be overexpressed in LSCC and correlated with advanced stage, and the inhibition of miR-21 suppresses cellular proliferation and invasion (3). miR-370 functions as a tumor suppressor via targeting Forkhead Box M1 in LSCC (11). miR-143-3p has also been extensively reported to be downregulated in various types of cancer and serves as a tumor suppressor by modulating cell proliferation, apoptosis, invasion and metastasis (12,13). However, the molecular mechanism underlying the function of miR-143-3p in the progression and development of LSCC remains to be elucidated.

Correspondence to: Dr Hua Cao, Ear Nose and Throat Hospital, The First Affiliated Hospital of Zhengzhou University, East 1 Jianshe Road, Zhengzhou, Henan 450052, P.R. China
E-mail: caohuachh@163.com

Key words: microRNAs, laryngeal squamous cell carcinoma, microRNA-143-3p, cell growth, metastasis, k-Ras/Raf/MEK/ERK pathway

k-Ras, a membrane-associated GTPase signaling protein, modulates cell survival, proliferation and differentiation (14). The k-Ras protein (21 kDa) located at the inner plasma membrane, is tightly correlated with the transduction of mitogenic signals (15). Accumulating evidence has demonstrated that k-Ras is important in tumorigenesis, cellular transformation and maintenance of a malignant phenotype (16-18). The ectopic expression of k-Ras has been found in various human tumors due to alterations in upstream or downstream signaling components or the triggering of mutations in RAS genes (19,20). The aberrant activation of downstream regulators in k-Ras pathways, including the RAF/mitogen-activated protein kinase kinase (MEK)/extracellular signal-regulated kinase (ERK) cascade, have been found to result in k-Ras-driven tumorigenesis, which is characterized by cellular transformation, metastasis and resistance to apoptosis (21-24). A previous study demonstrated that miR-21 increased the activation of oncogenic k-Ras and modulated non-small-cell lung cancer tumorigenesis via suppressing the negative regulators of the Ras/Raf/MEK/ERK pathway (25). In addition, Zhou *et al* reported that miR-30a suppresses tumor progression in hepatocellular carcinoma by inhibiting the Ras/Raf/MEK/ERK signaling pathway (26). Therefore, the miRNAs-mediated Ras/Raf/MEK/ERK pathway in LSCC requires further clarification.

The present study aimed to investigate miRNA expression profiles in the tumorigenesis of LSCC and examine the molecular mechanism underlying the biological function of miRNAs in the development of LSCC. The results revealed that miR-143-3p was downregulated in LSCC tissues and its expression predicted poor prognosis in LSCC. The findings also demonstrated that miR-143-3p repressed cell growth, migration and invasion in LSCC via modulating the k-Ras/Raf/MEK/ERK signaling pathway, and suggested that miR-143-3p may act as a tumor suppressor in LSCC tumorigenesis and represent a novel target for effective therapies.

Materials and methods

Patient tissue samples. Tumor tissues and matched normal tissues were obtained from 52 patients with LSCC at the Ear Nose and Throat Hospital, The First Affiliated Hospital of Zhengzhou University (Zhengzhou, China) between November, 2015 and January, 2016. The clinicopathological characteristics of the patients with LSCC are summarized in Table I. The tissues were collected from patients who had not received radiotherapy or chemotherapy prior to surgical resection. Verification of the specimens was performed by three pathologists according to the World Health Organization classification system (27). All patients provided written informed consent for the use of the tumor tissues for clinical investigation. All the tissues were snap-frozen in liquid nitrogen and stored at -80°C immediately following resection for subsequent experiments. The Institute Research Medical Ethics Committee of Zhengzhou University granted approval for the study.

Cell culture. The TU177, SNU899 and SNU46 human LSCC cell lines were purchased from the Cell Biology Institute of Shanghai, Chinese Academy of Science (Shanghai, China).

Human oral keratinocyte (HOK) cells (ScienCell Research Laboratories, Carlsbad, CA, USA) were used as a normal control (28). The LSCC cell lines were grown in RPMI-1640 (Gibco; Thermo Fisher Scientific, Inc., Waltham, MA, USA; cat. no. 11875) supplemented with 10% fetal bovine serum (FBS; Sigma; EMD Millipore, Billerica, MA, USA), 100 IU/ml penicillin and 100 mg/ml streptomycin (Invitrogen/Thermo Fisher Scientific, Inc.; cat. no. 15140-122), at 37°C in a humidified atmosphere containing 5% CO₂. The HOK cells were maintained in oral keratinocyte medium (ScienCell Research Laboratories) supplemented with oral keratinocyte growth supplement (ScienCell Research Laboratories).

Cell transfection. The miR-143-3p mimics/inhibitor and mimics/inhibitor negative control (NC) were designed and synthesized by Guangzhou RiboBio Co., Ltd. (Guangzhou, China). The cells were seeded into 6-well plates and transfected with miR-143-3p mimics/inhibitor and mimics/inhibitor NC (100 nM) using Lipofectamine 2000 (Invitrogen/Thermo Fisher Scientific, Inc.) according to the manufacturer's instructions. Following transfection for 48 h, the cells were collected for further measurements. The sequences are as follows: miR-143-3p mimics, 5'-UGAGAUGAAGCACUGUAGCUC-3'; miR-143-3p inhibitor, 5'-GAGCUACAGUGCUUCAUCUCA-3'; mimics NC, 5'-UUUGUACUACACAAAAGUACUG-3'; inhibitor NC, 5'-CAGUACUUUUGUGUAGUACAAA-3'.

miRNA microarray analysis. miRNA microarray analysis was performed to identify miRNA expression profiles in clinical samples. Total RNAs were extracted by TRIzol reagent (Invitrogen/Thermo Fisher Scientific, Inc.; cat. no. 15596-018), and the miRNA fraction was further purified using a mirVana miRNA isolation kit (Ambion; Thermo Fisher Scientific, Inc.; cat. no. AM1560) according to the manufacturer's protocol. The isolated miRNAs were labeled with Hy3 using the miRCURY array labeling kit (Exiqon, Inc., Vedbaek, Denmark; cat. no. 208032-A) and hybridized with miRCURY locked nucleic acid microRNA arrays (v8.0; Exiqon, Inc.). Microarray images were obtained using a Genepix 4000B scanner (Axon Instruments; Molecular Devices LLC, Sunnyvale, CA, USA) and analyzed with Genepix Pro 6.0 software (Axon Instruments; Molecular Devices LLC).

Reverse transcription-quantitative (RT-qPCR) analysis. Total RNA from the frozen tissues and cells were isolated using TRIzol reagent (Molecular Research Center, Inc., Cincinnati, OH, USA; cat. no. RT118) according to the manufacturer's protocol. 5 µl of RNA was reverse transcribed using a TaqMan Gene Expression Assays kit and TaqMan MicroRNA Reverse Transcription for k-Ras and miRNA according to the instructions of the manufacturer (Applied Biosystems/Thermo Fisher Scientific, Inc.). For analysis on a Step One Plus PCR machine (Applied Biosystems/Thermo Fisher Scientific, Inc.), 5 µl of cDNA was added to TaqMan® Fast Universal PCR Master Mix reagents (Applied Biosystems), to obtain final primer and probe concentrations of 300 nM/primer and 250 nM/probe in a 20 µl total volume. The sample was centrifuged briefly and run on the PCR machine using the default fast programme (40 cycles of 95°C for 1 sec, 60°C for 20 sec). GAPDH and U6 served as endogenous controls. The primer

Table I. Association between miR-143-3p and clinicopathological features of patients with laryngeal squamous cell carcinoma.

Clinicopathological parameter	Total n=52	miR-143-3p		P-value
		High (n)	Low (n)	
Sex				0.8967
Male	35	13	22	
Female	17	6	11	
Age (years)				0.8478
≤60	31	11	20	
>60	21	8	13	
T classification				0.0025
T1-2	24	14	10	
T3-4	28	5	23	
Differentiation				0.0041
G1	15	10	5	
G2	37	9	28	
Lymph node metastasis				0.0111
Negative	21	12	9	
Positive	31	7	24	
Primary location				0.9382
Supraglottic	25	9	16	
Glottic	27	10	17	
Clinical stage				0.0371
I-II	23	12	11	
III-IV	29	7	22	

Using the median of individual microRNA expression level as cut-off point, the LSCC cases were allocated into the high level and low level groups as regards the corresponding miRNA expression level. Pearson's Chi-square test was adopted to examine the association between the patient clinicopathological characteristics and each miRNA expression level. LSCC, laryngeal squamous cell carcinoma; miRNA or miR, microRNA.

sequences are as follows: miR-143-3p forward, 5'-UGAGAU GAAGCACUGUAGCUC-3', reverse, 5'-GTCGTATCCAGTGC GTGTCTCGTG-3'; k-Ras forward, 5'-ACTGAATATAAACCT TGTGGTAG-3', reverse, 5'-TCAAAGAATGGTCCTGGACC-3'; GAPDH forward, 5'-TGTGGGCATCAATGGATTTGG-3', reverse, 5'-ACACCATGTATTCCGGGTCAAT-3'; U6 forward, 5'-CTCGCTTCGGCAGCAC-3', reverse, 5'-AACGCTTCA CGAATTTGCGT-3'. The relative quantification ($2^{-\Delta\Delta C_t}$) method (29) was used to calculate fold changes.

Cell viability analysis. Cell viability was measured using a Cell Counting Kit-8 (CCK-8) assay according to the manufacturer's protocol. Briefly, the cells (5×10^4 cells/well) were seeded in 96-well plate with 100 μ l RPMI-1640 medium supplemented with 10% FBS. Then, 10 μ l of CCK-8 solution (Dojindo Molecular Technologies, Inc., Gaithersburg, MD, USA) was added into each well and the mixture was incubated for 1 h at 37°C with 5% CO₂. The absorbance rate at 450 nm was

measured using a microplate reader (Bio-Rad Laboratories, Inc., Hercules, CA, USA). Each experiment was repeated at least three times.

Analysis of apoptosis. Flow cytometric analysis was used to measure cell apoptosis. The cells (1×10^6 cells) were harvested and washed twice with cold PBS. The cells were then fixed with 70% ice-cold methanol at 4°C for 30 min. Following two PBS washes, the cells were resuspended in binding buffer and incubated with 5 μ l of Annexin V-FITC (BD Biosciences, Franklin Lakes, NJ, USA) and 1 μ l of propidium iodide (PI; 50 μ g/ml; BD Biosciences). Flow cytometric analysis was performed within 5 min. All samples were analyzed by flow cytometry (FACSCalibur; BD Biosciences).

Western blot analysis. The cells were lysed as described previously (30). The BCA protein assay kit (Pierce; Thermo Fisher Scientific, Inc.) was used to measure protein concentration. The protein samples (60 μ g) were separated in 10% SDS-polyacrylamide gels (Sigma-Aldrich; EMD Millipore) and then transferred onto polyvinylidene difluoride membranes (BD Pharmingen, San Diego, CA, USA). The membranes were then blocked with 5% skim milk at room temperature for 1 h, and were incubated primary antibodies at 4°C overnight against cleaved-caspase-3 (1:1,000; cat. no. SC-5298; Santa Cruz Biotechnology, Inc., Dallas, TX, USA), B cell lymphoma 2 (Bcl-2; 1:1,000; cat. no. SC-492; Santa Cruz Biotechnology, Inc.), Bcl-2-associated X protein (Bax; 1:500; cat. no. SC-526; Santa Cruz Biotechnology, Inc.), E-cadherin (1:1,000; cat. no. SC-7870; Santa Cruz Biotechnology, Inc.), N-cadherin (1:1,000; cat. no. SC-7939; Santa Cruz Biotechnology, Inc.), Vimentin (1:1,000; cat. no. SC-5565; Santa Cruz Biotechnology, Inc.), matrix metalloproteinase (MMP-9; 1:1,000; cat. no. SC-12759; Santa Cruz Biotechnology, Inc.), k-Ras (1:1,000; cat. no. SC-30; Santa Cruz Biotechnology, Inc.), phosphorylated (p)-Raf/1 (1:1,000; cat. no. ab130572; Abcam, Cambridge, UK), Raf/1 (1:1,000; cat. no. ab137435; Abcam), p-MEK1/2 (1:1,000; cat. no. SC-436; Santa Cruz Biotechnology, Inc.), MEK1/2 (1:1,000; cat. no. 9154S; Cell Signaling Technology, Inc., Danvers, MA, USA), p-ERK1/2 (1:1,000; cat. no. SC-81492; Santa Cruz Biotechnology, Inc.) and ERK1/2 (1:1,000; cat. no. SC-514302; Santa Cruz Biotechnology, Inc.). β -actin (1:750; cat. no. A5060; Sigma-Aldrich; EMD Millipore) served as an internal control. The membranes were then incubated for 2 h with horseradish peroxidase-conjugated antibodies (1:1,000; cat. no. SC-2060; Santa Cruz Biotechnology, Inc.) at room temperature. Subsequently, the protein bands were scanned on the X-ray film using the enhanced chemiluminescence detection system (PerkinElmer, Inc., Boston, MA, USA). The Alpha Imager software 2000 (Alpha Innotech Corporation, San Leandro, CA, USA) was performed to measure the relative intensity of each band on the western blots.

Xenograft tumor model. All animal procedures were approved by the Animal Care Committee of the Zhengzhou University. The female BALB/C athymic nude mice (7-8 weeks old; n=20; weighing 26 ± 4 g) were obtained from Cancer Institute of the Chinese Academy of Medical Science. The mice were housed in laminar flow cabinets under specific pathogen-free

conditions, and fed *ad libitum*. The mice were housed on 12:12-h light–dark cycle in a temperature controlled ($24\pm 2^{\circ}\text{C}$) and humidity-controlled room, with free access to standard chow and tap water. Overall, 1×10^7 BGC-823 cells in 200 μl of sterile PBS were administered to the BALB/c nude mice by subcutaneous injection. The female BALB/C athymic nude mice (7–8 weeks; $n=4$) were inoculated with SNU899 and SNU46 (1×10^7 cells in 200 μl of sterile PBS) transfected with miR-143-3p mimic or mimic negative control (NC) in the forelimb. The tumor cells were allowed to grow for 4 weeks. The tumors were then excised and weighed from the sacrificed mice at 28 days.

Cell invasion assay. Cell invasion assays were performed using 24-well Transwell chambers with an 8.0- μm pore size polycarbonate membrane (Corning Incorporated, Corning, NY, USA). The TU177 and SNU899 cells were seeded on the upper surface of the membrane precoated with Matrigel (BD Biosciences). Subsequently, the non-invading cells on the upper side of the membrane were removed and invading cells on the lower surface of the membrane were fixed with methanol and stained with crystal violet (cat. no. MAK083; Sigma-Aldrich; EMD Millipore). The cell numbers were counted under a microscope (Olympus IX81, Olympus Corp., Tokyo, Japan; magnification, $\times 100$).

Cell migration assay. The wound-healing assay was used to examine cell migration. The TU177 and SNU899 cells were plated onto 6-well plates. The cells were serum-starved overnight prior to wounding of the monolayers by scratching with a 10- μl micropipette pipette tip. Following 48 h of incubation, the migration status was examined by measuring the movement of cells into the scraped area. Images were captured at different points of time post-wounding. The wound area was measured and the percentage of closure of the denuded area was counted using Image J software (Version 1.42q, National Institutes of Health, Bethesda, MD, USA).

Luciferase assay. The potential binding site between k-Ras and miR-143-3p was searched using TargetScan (<http://www.targetscan.org>). The miR-143-3p mimics/inhibitor and corresponding NC were synthesized by Guangzhou RiboBio Co., Ltd. The wild-type k-Ras-3'-UTR (WT) and mutant k-Ras-3'-UTR (mut) containing the putative binding site of miR-143-3p were established (Fig. 4A) and cloned into the firefly luciferase expressing vector pMIR-REPORT (Ambion; Thermo Fisher Scientific, Inc.). Site-directed mutagenesis of the k-Ras 3'-UTR at the putative miR-143-3p binding site was performed using a QuikChange kit (Qiagen, Inc., Valencia, CA, USA). For the luciferase assay, TU177 cells (2×10^5 per well) were seeded into 24-well plates and co-transfected with 0.8 μg of pMIR-k-Ras-3'-UTR or pMIR-k-Ras-mut-3'-UTR, 50 nM miR-143-3p mimic/inhibitor or mimic NC using Lipofectamine 2000 reagent (cat. no. 11668-027; Invitrogen/Thermo Fisher Scientific, Inc.). The ratio of Firefly to *Renilla* was used to normalize the relative Firefly luciferase activity 48 h following transfection, and measured with the Dual-Light luminescent reporter gene assay (Applied Biosystems; Thermo Fisher Scientific, Inc.).

Immunohistochemistry. Immunohistochemistry was performed on paraformaldehyde-fixed paraffin sections (5 μm thickness). The tissue slides were deparaffinized with xylene and rehydrated with graded series of ethanol. Following antigen retrieval, the sections were blocked with bovine serum (Gibco/Thermo Fisher Scientific, Inc., 10%) in PBS for 30 min and incubated overnight at 4°C with the following primary antibodies: Anti-k-Ras (1:500; cat. no. SC-30; Santa Cruz Biotechnology, Inc.), anti-p-Raf/1 (1:500; cat. no. ab130572; Abcam) and anti-p-ERK1/2 (1:500; cat. no. SC-81492; Santa Cruz Biotechnology, Inc.). The sections were then incubated overnight at 4°C with secondary antibodies (IgG antibodies; 1:1,000; cat. no. SC-2060; Santa Cruz Biotechnology, Inc.). The immunostaining was visualized with diaminobenzidine (cat. no. D5637; DAB; Sigma; EMD Millipore) for 3 min, covered with a cover-slip, and analyzed under a light microscope.

Statistical analysis. All statistical analyses were performed using SPSS software (version 19.0; IBM SPSS, Armonk, NY, USA). Data were obtained from independent experiments repeated at least three times. Numerical data are presented as the means \pm standard deviation. The association between the clinicopathological characteristics of the patients with LSCC and miR-143-3p low and high expression was determined by the Pearson's Chi-square test. Independent t-tests were used to compare differences between 2 groups. One-way ANOVA with Tukey's post hoc tests were performed to compare the differences between 3 or more groups. Kaplan-Meier curve analysis with a log-rank test was used to evaluate the survival rate between patients with high- and low-miR-143-3p expressing tumors. The correlation between k-Ras and miR-143-3p expression levels was determined by with Pearson's correlation analysis. $P<0.05$ was considered to indicate a statistically significant difference.

Results

miR-143-3p is downregulated in LSCC tissues and is negatively associated with the patient survival rate. To determine the expression of miRNAs involved in LSCC tumorigenesis, microarray analysis was used to determine miRNA levels in LSCC tissues and matched normal tissues. As shown in Fig. 1A, compared with the normal tissues, several miRNAs were altered in tumor tissues, with the most marked significant downregulation in miR-143-3p. Several studies have demonstrated that miR-143-3p is downregulated in cancer tissues and functions as a tumor suppressor in various types of cancer, including esophageal cancer and breast cancer (12,13). However, the role of miR-143-3p in LSCC remains to be elucidated. Therefore, the present study investigate the role of miR-143-3p in the development of LSCC. Consistent with the microarray analysis results, the RT-qPCR analysis further confirmed that the levels of miR-143-3p were significantly downregulated in cancer tissues ($n=52$) compared with control tissues ($P<0.01$; Fig. 1B). Previous studies have reported that the development of tumors is associated with the clinicopathological features, including T classification, differentiation and lymph node metastasis, in patients (31–33). Therefore, the present study further analyzed the association between miR-143-3p and the clinicopathological features of patients with LSCC (Table I). It was observed that a low

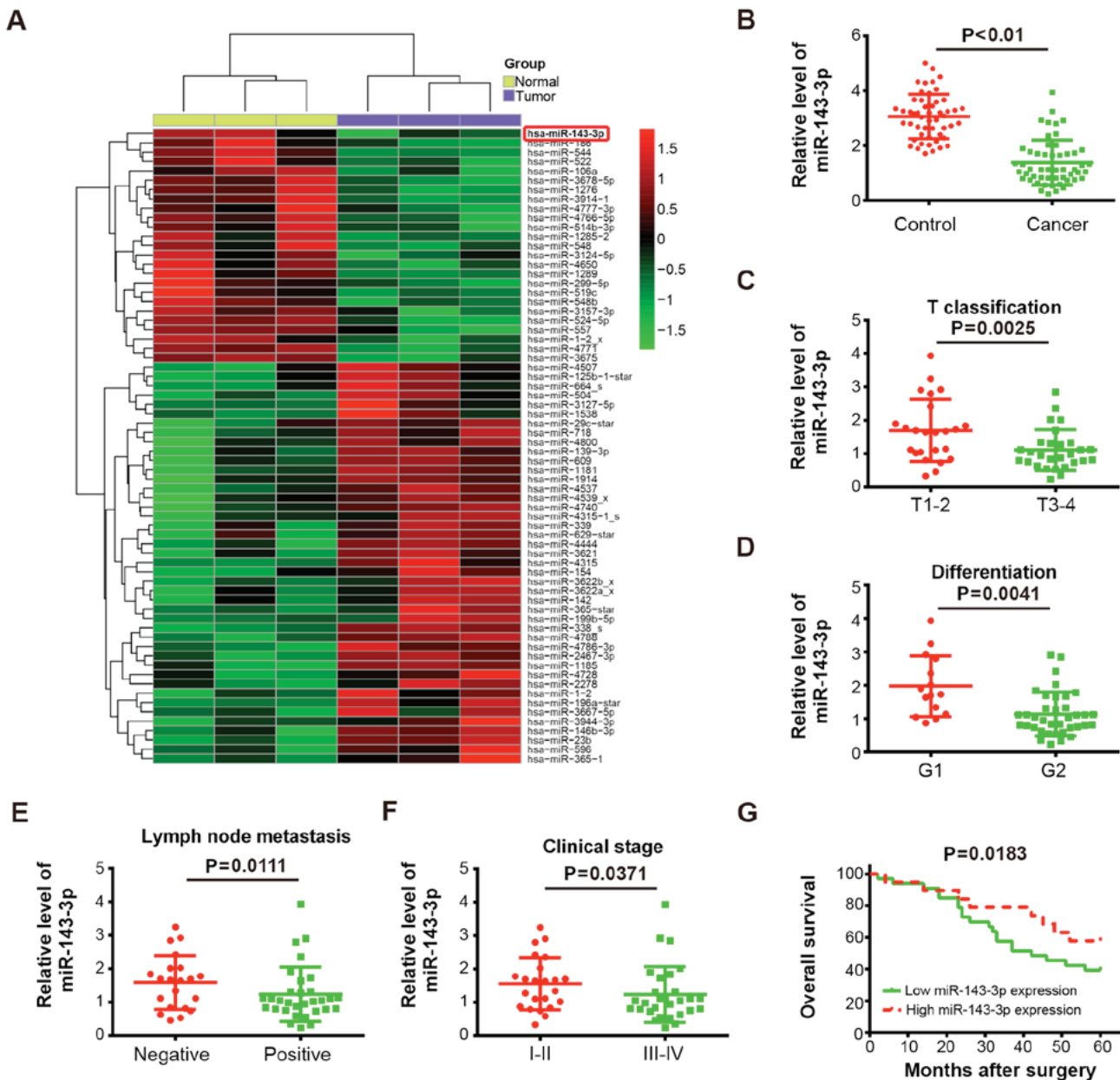


Figure 1. miR-143-3p is downregulated in LSCC tissues and correlates with tumor progression. (A) Microarray analysis was performed to determine the miRNA expression profiles in LSCC tissues and matched normal tissues. The color code is linear within the heat map; green represents the lowest level of expression and red the highest. (B) RT-qPCR analysis was used to measure the expression of miR-143-3p in LSCC tissues and matched normal tissues (n=52) (P<0.01). RT-qPCR analysis was performed to detect the level of miR-143-3p in tumor tissues, grouped according to clinicopathological features of patients with LSCC (C) T classification (P=0.0025), (D) differentiation (P=0.0041), (E) lymph node metastasis (P=0.0111) and (F) clinical stage (P=0.0371). (G) Kaplan-Meier survival analysis was performed to investigate the correlation between the expression of miR-143-3p and patient prognosis (P=0.0183). Data are presented as the means \pm standard deviation of three individual experiments. LSCC, laryngeal squamous cell carcinoma; miRNA/miR, microRNA; RT-qPCR, reverse transcription-quantitative polymerase chain reaction.

expression of miR-143-3p was negatively associated with T classification (P=0.0025; Fig. 1C), differentiation (P=0.0041; Fig. 1D), lymph node metastasis (P=0.0111; Fig. 1E) and clinical stage (P=0.0371; Fig. 1F) in patients with LSCC. However, there was no associated between the expression of miR-143-3p and patient gender, age or primary location (Table I). To assess the correlation between the expression of miR-143-3p and the prognosis of patients with LSCC, Kaplan-Meier survival analysis was used to evaluate the LSCC survival curves. It was observed that patients with low expression of miR-143-3p (n=33) had a lower overall survival

percentage, compared with those with high expression of miR-143-3p (n=19; P=0.0183; Fig. 1G). Collectively, these results demonstrated that miR-143-3p was downregulated in LSCC tissues and a low expression of miR-143-3p predicts poor prognosis in LSCC, suggesting that miR-143-3p may function as a tumor suppressor in LSCC tumorigenesis.

Overexpression of miR-143-3p inhibits LSCC cell proliferation, induces apoptosis in vitro and suppresses tumor growth in vivo. To further examine the functions of miR-143-3p in LSCC cells, the levels of miR-143-3p were measured

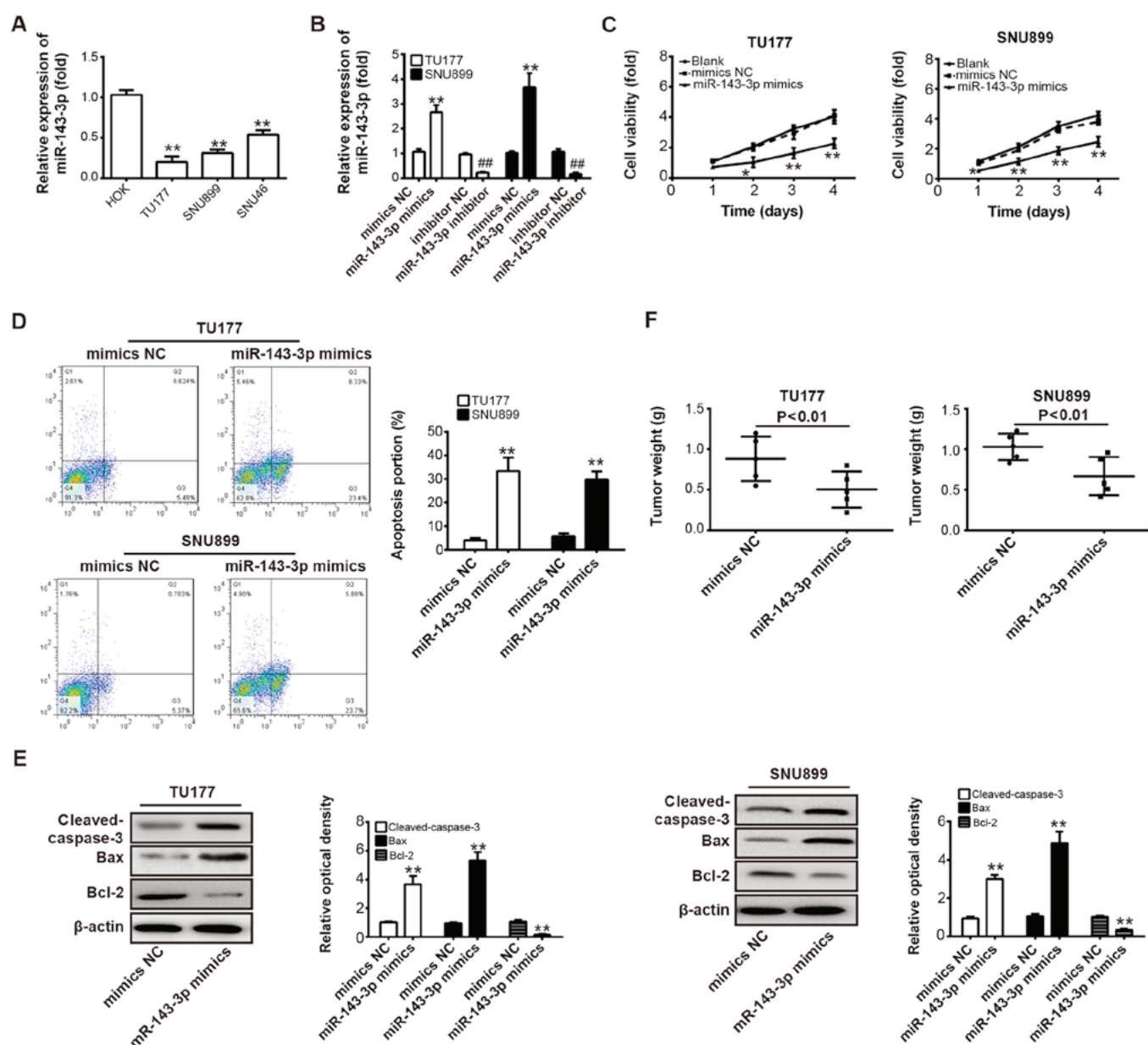


Figure 2. Overexpression of miR-143-3p represses LSCC cell proliferation, induces apoptosis and suppresses tumor growth. (A) Expression of miR-143-3p was measured using RT-qPCR analysis in TU177, SNU899 and SNU46 LSCC cell lines, and HOK normal epithelial cell lines. **P<0.01 vs. HOK. (B) RT-qPCR analysis was used to determine the level of miR-143-3p in TU177 and SNU899 cells transfected with miR-143-3p mimics/inhibitor or NC mimics/inhibitor. **P<0.01 vs. NC mimics; #P<0.01 vs. NC inhibitor. (C) A Cell Counting Kit-8 assay was performed to measure cell viability in TU177 and SNU899 cells transfected with miR-143-3p mimics or NC mimics. *P<0.05 and **P<0.01 vs. NC mimics. (D) TU177 and SNU899 cells were transfected with miR-143-3p mimics or NC mimics and cell apoptosis was determined by flow cytometric analysis. **P<0.01 vs. NC mimics. (E) Cleaved-caspase-3, Bax and Bcl-2 were detected in TU177 and SNU899 cells transfected with miR-143-3p mimics or NC mimics. β -actin was used as an internal control for protein loading. **P<0.01 vs. NC mimics. (F) Xenograft model was injected with miR-143-3p-overexpressing TU177 or SNU899 cells and tumor growth was determined by measuring tumor weight (n=5/group). Data are presented as the means \pm standard deviation of three individual experiments. **P<0.01 vs. NC mimics. LSCC, laryngeal squamous cell carcinoma; miR, microRNA; RT-qPCR, reverse transcription-quantitative polymerase chain reaction; Bcl-2, B-cell lymphoma 2; Bax, Bcl-2-associated X protein; NC, negative control.

in TU177, SNU899 and SNU46 LSCC cell lines, and HOK cells. As shown in Fig. 2A, the expression of miR-143-3p was significantly downregulated in all LSCC cell lines compared with the normal epithelial cell lines (P<0.01). Based on these data, the two LSCC cells (TU177 and SNU899) with the lowest expression level of miR-143-3p were selected for further experiments. The TU177 and SNU899 cells were transfected with miR-143-3p mimics/inhibitor or mimics/inhibitor NC, and the transfection efficiency of miR-143-3p mimics/inhibitor were evaluated by RT-qPCR analysis. As shown in Fig. 2B,

miR-143-3p was significantly downregulated or upregulated in these TU177 and SNU899 cells, compared with the cells transfected with mimics/inhibitor NC (P<0.01). Subsequently, the CCK-8 assay and flow cytometric analysis were performed to measure cell viability and apoptosis in TU177 and SNU899 cells following transfection with miR-143-3p mimics or NC mimics, respectively. It was found that the overexpression of miR-143-3p markedly reduced cell viability and increased apoptotic cells compared with the control (P<0.01; Fig. 2C and D). To further examine the molecular

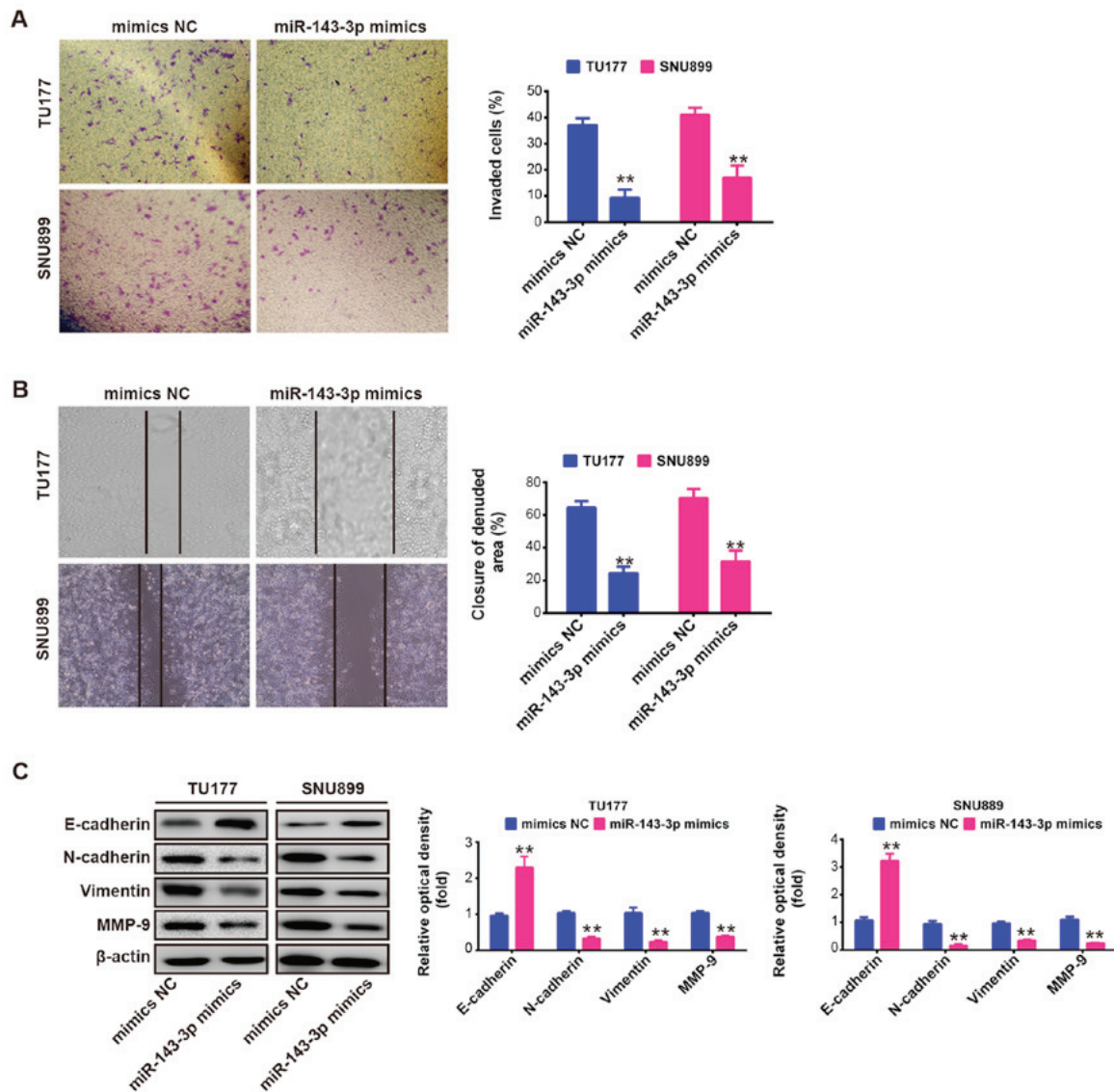


Figure 3. Overexpression of miR-143-3p suppresses cell migration and invasion. (A) Transwell invasion assay (magnification, x100) to evaluate the cell invasion in TU177 and SNU899 cells transfected with miR-143-3p mimics or NC mimics. (B) Wound-healing assay was used to determine cell migration in TU177 and SNU899 cells following transfection with miR-143-3p mimics or NC mimics. (C) TU177 and SNU899 cells were transfected with miR-143-3p mimics or NC mimics, and the expression levels of E-cadherin, N-cadherin, vimentin and MMP-9 were measured using western blot assays. β-actin served as an internal control for protein loading. Data are presented as the means ± standard deviation of three individual experiments. **P<0.01, vs NC mimics. miR, microRNA; NC, negative control; MMP, matrix metalloproteinase.

mechanisms of miR-143-3p-induced apoptosis, western blot analysis was used to determine the expression levels of apoptosis-related proteins in TU177 and SNU899 cells transfected with miR-143-3p mimics or NC mimics. It was found that the overexpression of miR-143-3p significantly increased the protein expression of pro-apoptotic cleaved-caspase-3 and Bax, and decreased the protein expression of anti-apoptotic Bcl-2, compared with the NC mimics (P<0.01; Fig. 2E). To investigate whether the overexpression of miR-143-3p influences tumorigenesis *in vivo*, a xenograft mouse model was established, which was subcutaneously injected with miR-143-3p-overexpressing TU177 or SNU899 cells and their parallel NC mimics-carrying cells. Following injection, the tumor growth was determined by measuring the weight. It was found that the miR-143-3p-overexpressing cells exhibited a significant decrease in the tumor weight compared with the control cells (P<0.01; Fig. 2F). These data indicated that the

overexpression of miR-143-3p possessed antitumor effects via inhibiting cell proliferation and inducing apoptosis *in vitro*, and repressing tumor growth *in vivo*.

Overexpression of miR-143-3p inhibits cell migration and invasion in vitro. The present study further evaluated the effects of the upregulation of miR-143-3p on cell invasion and migration, which are key factors in malignant progression and metastasis. The TU177 and SNU899 cells were transfected with miR-143-3p mimics or NC mimics, and cell invasion was evaluated using a Transwell invasion assay. As shown in Fig. 3A, the invaded cells were significantly inhibited by the overexpression of miR-143-3p compared with the NC mimics (P<0.01). Subsequently, a wound-healing assay was performed to determine cell migration following transfection with miR-143-3p mimics or NC mimics. It was observed that the overexpression of miR-143-3p also markedly suppressed

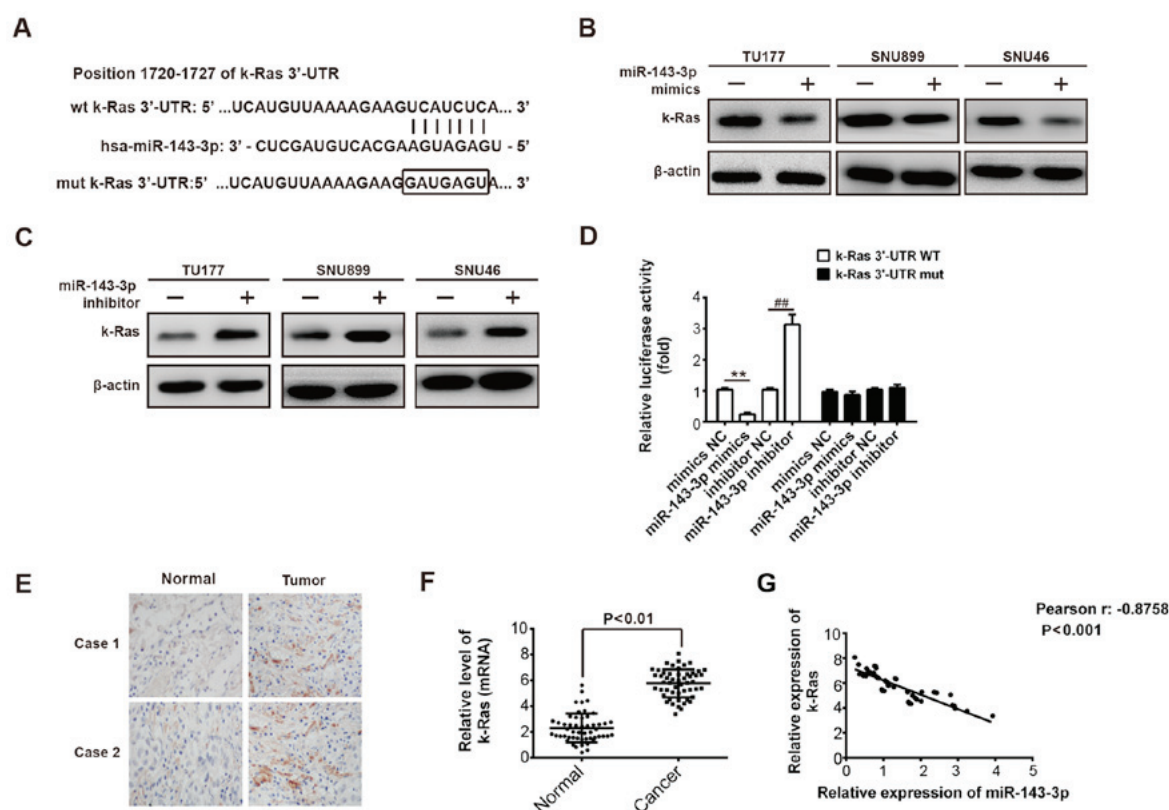


Figure 4. miR-143-3p inhibits expression of k-Ras by directly targeting its 3'-UTR. (A) k-Ras 3'-UTR containing the wt or mut binding site for miR-143-3p. (B) Western blot analysis was performed to detect levels of k-Ras in three LSCC cells (TU177, SNU899 and SNU46) following transfection with miR-143-3p mimics or NC mimics. β -actin served as an internal control. (C) Western blot analysis was used to measure the expression of k-Ras in three LSCC cells (TU177, SNU899 and SNU46) transfected with miR-143-3p inhibitor or NC inhibitor. β -actin served as an internal control. (D) Relative luciferase activity of k-Ras wt or mut 3'-UTR in TU177 cells following transfection with the miR-143-3p mimic/inhibitor or corresponding NC. ** P <0.01, vs NC mimic. ## P <0.01, vs NC inhibitor. (E) Representative images of immunohistochemical staining of k-Ras in LSCC and adjacent normal tissues. (F) Levels of miR-143-3p were measured using reverse transcription-quantitative polymerase chain reaction analysis in the LSCC and matched normal tissues ($n=52$). ** P <0.01, vs normal tissues. (G) Negative correlation between k-Ras and miR-143-3p levels in patients with LSCC ($r=-0.8758$, $P<0.001$). Data are presented as the means \pm standard deviation of three individual experiments. LSCC, laryngeal squamous cell carcinoma; miR, microRNA; wt, wild-type; mut, mutant.

the migration of TU177 and SNU899 cells ($P<0.01$; Fig. 3B). These results suggested that the overexpression of miR-143-3p suppressed cell migration and invasion *in vitro*, although the potential molecular mechanism requires further investigation for a deeper understanding.

It is well reported that tumor cell invasion and metastasis are tightly correlated with several processes, including epithelial-mesenchymal transition (EMT), matrix metalloproteinase (MMP) upregulation and adhesion molecule downregulation in cancer cells. Epithelial tumor progression to more aggressive metastatic tumors, concurrent upregulation of mesenchymal protein markers N-cadherin and vimentin, and loss of epithelial protein marker E-cadherin are important cellular events during EMT (34-36). E-cadherin, an EMT marker, is frequently downregulated in various tumors, including LSCC (37,38), and loss of its function or expression decreases cell-cell contacts and results in tumor invasion and metastasis (39). MMP-9, a member of the MMP family, is expressed at a high level in cancer tissues, and is correlated with the processes of tumor metastasis and invasion in human cancer, including LSCC (40,41). Studies have demonstrated that EMT and MMP-9 in different types of cancer are regulated by post-transcriptional mechanisms, including miRNAs (40,42). Therefore, to further elucidate the molecular mechanism

by which the overexpression of miR-143-3p suppresses cell migration and invasion *in vitro*, the TU177 and SNU899 cells were transfected with miR-143-3p mimics or NC mimics, and the expression levels of E-cadherin, N-cadherin, vimentin and MMP-9 were measured by western blot assays. As shown in Fig. 3C, the overexpression of miR-143-3p increased the protein level of E-cadherin, but decreased the levels of N-cadherin, vimentin and MMP-9 in the TU177 and SNU899 cells. Taken together, these data indicated that the overexpression of miR-143-3p suppressed cell migration and invasion through regulating EMT and MMP-9.

miR-143-3p inhibits the expression of k-Ras by targeting its 3'-UTR. There is increasing evidence that k-Ras acts as an oncogene via regulating tumorigenesis and cellular transformation in various types of cancer (16,17,43). A previous study reported that miR-143-3p serves as a tumor suppressor via targeting oncogene k-Ras in renal cell carcinoma (44). To determine whether k-Ras is a target of miR-143-3p in LSCC cells, bioinformatics analysis was performed to predicate the putative targets of miR-143-3p, and it was found that k-Ras may be a target gene of miR-143-3p (Fig. 4A). To investigate whether the expression of k-Ras is controlled by miR-143-3p, the TU177, SNU899 or SNU46 LSCC cell lines were transfected

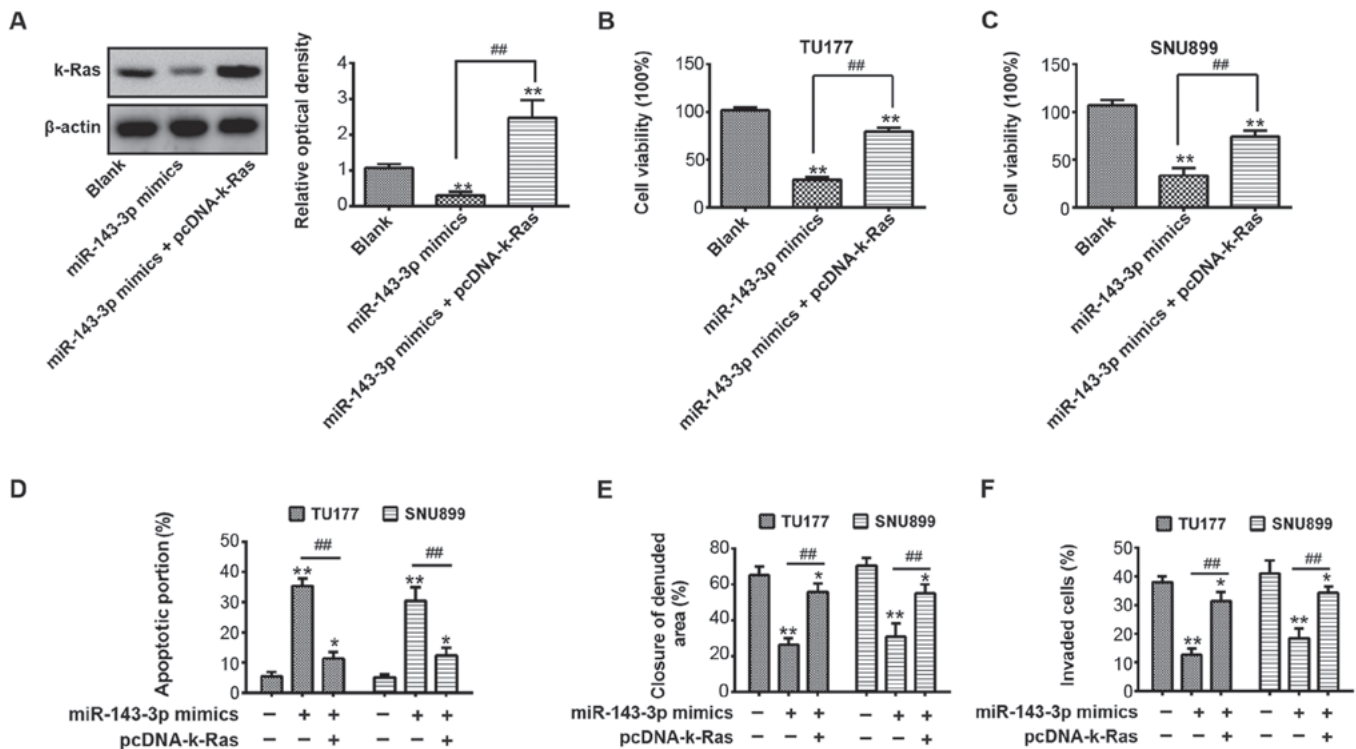


Figure 5. Suppressive effects of miR-143-3p on laryngeal squamous cell carcinoma cells are rescued by overexpression of k-Ras. TU177 or SNU899 cells were transfected with miR-143-3p mimics or were co-transfected with miR-143-3p mimics and the pcDNA-k-Ras plasmid. (A) Expression of k-Ras was measured in TU177 cells using western blot analysis. β -actin served as an internal control. $^{**}P<0.01$, vs. blank group. $^{##}P<0.01$, vs. miR-143-3p mimics group. A Cell Counting-Kit-8 assay was used to determine the cell viability of (B) TU177 and (C) SNU899 cells. $^{**}P<0.01$, vs. blank group. $^{##}P<0.01$, vs. miR-143-3p mimics group. (D) Cell apoptosis was measured by flow cytometry in TU177 or SNU899 cells. $^{*}P<0.05$ and $^{**}P<0.01$, vs. blank group. $^{##}P<0.01$, vs. miR-143-3p mimics group. (E) Wound-healing assay was performed to evaluate the cell migration of TU177 or SNU899 cells. $^{*}P<0.05$ and $^{**}P<0.01$, vs. blank group. $^{##}P<0.01$, vs. miR-143-3p mimics group. (F) Transwell invasion assay was used to measure the cell invasion of TU177 or SNU899 cells. $^{*}P<0.05$ and $^{**}P<0.01$, vs. blank group. $^{##}P<0.01$, vs. miR-143-3p mimics group. Data are presented as the means \pm standard deviation of three individual experiments. miR, microRNA.

with mimics/inhibitor or NC, and the protein level of k-Ras was determined using western blot analysis. It was found that the expression of k-Ras was decreased by the overexpression of miR-143-3p (Fig. 4B), whereas the knockdown of miR-143-3p increased the protein level of k-Ras in all LSCC cells, compared with the level in the NC group (Fig. 4C). To validate whether the k-Ras is the direct target of miR-143-3p, luciferase-reporter plasmids were constructed containing the WT or mut 3'-UTR segments of k-Ras (Fig. 4A). The WT or mut reporter plasmid was co-transfected into TU177 cells with miR-143-3p mimics/inhibitor or NC, and the luciferase activity was measured. The results showed that the miR-143-3p mimic markedly repressed the luciferase activity compared with the NC mimic, whereas the miR-143-3p inhibitor increased the luciferase activity compared with the NC inhibitor in the presence of the WT 3'-UTR ($P<0.01$; Fig. 4D). miR-143-3p did not suppress the luciferase activity of the reporter vector containing the 3'-UTR of k-Ras with mutations in the miR-143-3p-binding site (Fig. 4D). These data indicated that k-Ras is a direct target of miR-143-3p in LSCC cells.

To further clarify the association between miR-143-3p and k-Ras in LSCC, immunohistochemistry and RT-qPCR assays were performed to detect the expression of k-Ras in the 52 paired LSCC and matched normal tissues. It was observed that the 52 cases of tumors showed enhanced expression of k-Ras when compared with adjacent normal tissues ($P<0.01$; Fig. 4E and F). Correlation analysis showed that the expression

levels of k-Ras in tumor tissues were inversely correlated with the levels of miR-143-3p ($r=-0.8758$, $P<0.001$; Fig. 4G). These results suggested that miR-143-3p negatively modulated the expression of k-Ras and their inverse correlation was determined in clinical samples.

Overexpression of k-Ras rescues the suppressive effects of the upregulation of miR-143-3p on LSCC cells. To further investigate whether the ectopic expression of k-Ras rescued the suppressive effect of miR-143-3p, the TU177 and SNU899 cells were transfected with miR-143-3p mimics or were co-transfected with miR-143-3p mimics and the pcDNA-k-Ras plasmid. Cells without transfection are used as a control (blank group). The results showed that the overexpression of miR-143-3p significantly decreased the expression of k-Ras compared with the blank group, however, the pcDNA-k-Ras plasmid led to marked k-Ras upregulation compared with the miR-143-3p mimics group ($P<0.01$; Fig. 5A). Subsequently, cell viability, apoptosis, migration and invasion in each group were measured using a CCK-8 assay, flow cytometry, a wound-healing assay and Transwell invasion assay, respectively. It was found that the overexpression of miR-143-3p inhibited cell proliferation, migration and invasion, and promoted apoptosis, however, the upregulation of k-Ras led to a marked increase in cell proliferation, migration and invasion, and decrease in apoptosis in the TU177 and SNU899 cells following co-transfection with miR-143-3p mimics

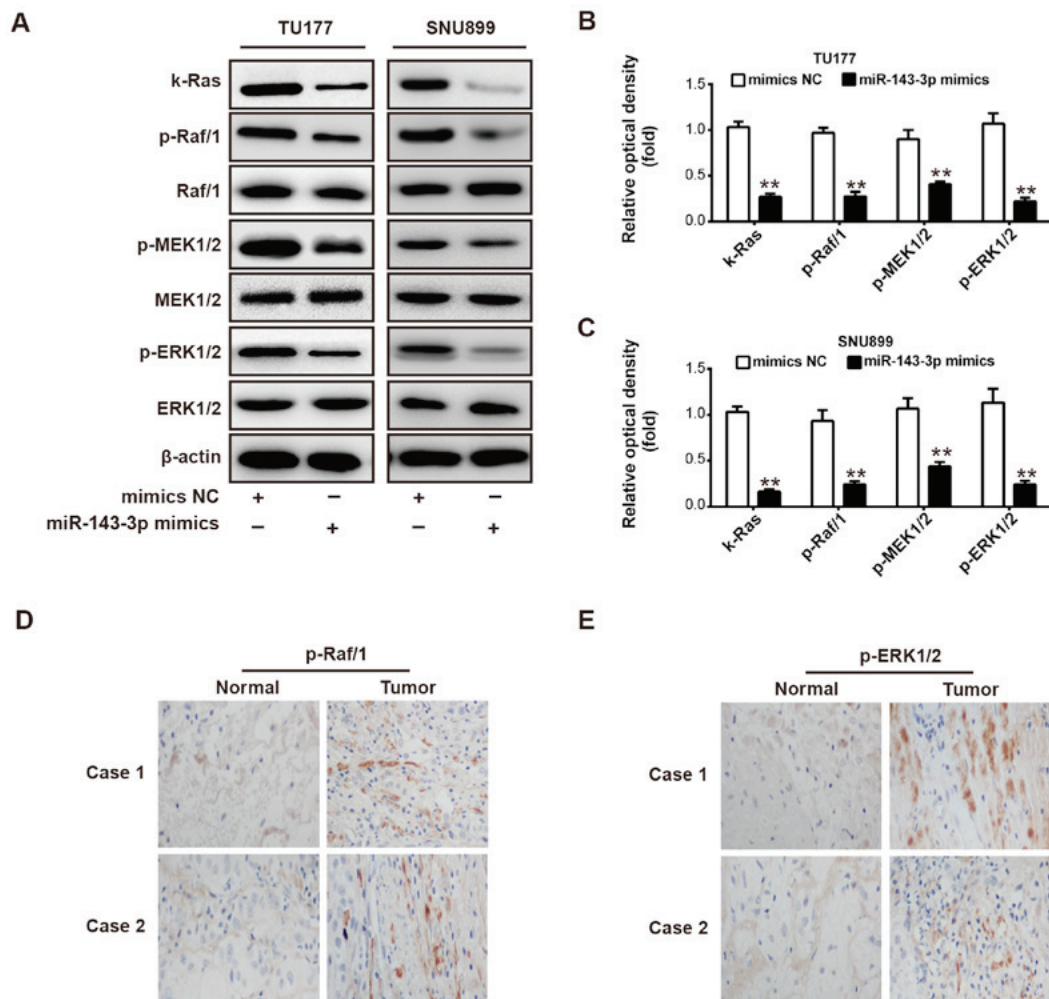


Figure 6. miR-143-3p modulates the k-Ras/Raf/MEK/ERK signaling pathway. (A) TU177 and SNU899 cells were transfected with miR-143-3p mimic or NC mimic, and western blot analysis was used to detect the expression of k-Ras, Raf/1, MEK1/2 and ERK1/2. Levels of k-Ras, Raf/1, MEK1/2 and ERK1/2 are shown in bar graphs for (B) TU177 and (C) SNU899 cells, respectively. Immunohistochemistry assays were used to detect the expression of (D) p-Raf/1 and (E) p-ERK1/2 in laryngeal squamous cell carcinoma and adjacent normal tissues, respectively (magnification, $\times 100$). Data are presented as the mean \pm standard deviation of three individual experiments. ** $P < 0.01$, vs. NC. miR, microRNA; NC, negative control; MEK, mitogen-activated protein kinase; ERK, extracellular signal-regulated kinase; p-, phosphorylated.

and the pcDNA-k-Ras plasmid ($P < 0.01$; Fig. 5B-F). These results indicated that the suppressive effects of miR-143-3p on cell growth, migration and invasion were rescued by the overexpression of k-Ras in LSCC cells.

miR-143-3p suppresses the k-Ras/Raf/MEK/ERK signaling pathway. The k-Ras/Raf/MEK/ERK intracellular signaling pathway is involved in the regulation of diverse cellular functions, including survival, proliferation, apoptosis, motility and metabolism (45,46). A previous study reported that miR-221 inhibits cell proliferation in endothelial progenitor cells via modulating the Raf/MEK/ERK pathway (47). The present study examined whether the aberrant expression of miR-143-3p regulates the Raf/MEK/ERK signaling pathway via targeting k-Ras in LSCC cells. To confirm this hypothesis, the TU177 and SNU899 cells were transfected with miR-143-3p mimic or NC mimic, and western blot analysis was performed to detect the levels of k-Ras, Raf/1, MEK1/2 and ERK1/2. As shown in Fig. 6A-C, the overexpression of miR-143-3p significantly inhibited the expression of p-k-Ras, p-Raf/1, p-MEK1/2 and p-ERK1/2 in the TU177 and SNU899 cells compared with the

NC mimic ($P < 0.01$). The previous results demonstrated that miR-143-3p was downregulated in LSCC tissues. To confirm whether the lower expression of miR-143-3p is associated with augmented expression of Raf/1 and ERK1/2 in LSCC, clinical tumor samples were collected for the immunohistochemistry assay. As shown in Fig. 6D and E, a lower expression of miR-143-3p in LSCC tissues was associated with increased expression of p-Raf/1 and p-ERK1/2. These data suggested that miR-143-3p may suppress cell growth, migration and invasion in LSCC via repressing the k-Ras/Raf/MEK/ERK signaling pathway.

Downregulation of miR-143-3p suppresses the mitochondrial apoptotic pathway and induces the EMT cascade. Our data provided direct evidence that miR-143-3p was downregulated in LSCC tissues and that a low expression of miR-143-3p predicts the poor prognosis of patients with LSCC, suggesting that miR-143-3p may serve as a potential prognostic biomarker and therapeutic target. The downregulation of miR-143-3p in LSCC resulted in k-Ras, p-Raf/1, p-MEK1/2 and p-ERK1/2 upregulation, inhibited the mitochondrial apoptotic pathway

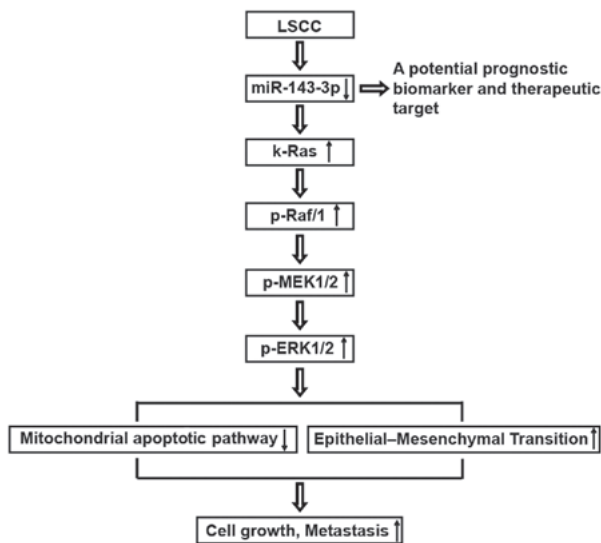


Figure 7. Schematic diagram of the regulatory and signaling network of miR-143-3p in LSCC. The schematic diagram illustrates the inducing effect of miR-143-3p on the k-Ras/Raf/MEK/ERK signaling pathway in LSCC. Downregulation of miR-143-3p in LSCC induces the upregulation of k-Ras, p-Raf/1, p-MEK1/2 and p-ERK1/2, inhibits the mitochondrial apoptotic pathway and activates the epithelial-mesenchymal transition cascade, which is involved in diverse cellular responses, including cell growth and metastasis. LSCC, laryngeal squamous cell carcinoma; miR, microRNA; MEK, mitogen-activated protein kinase; ERK, extracellular signal-regulated kinase; p-, phosphorylated.

and activated the EMT cascade, which is associated diverse cellular responses, including cell growth and metastasis (Fig. 7).

Discussion

miRNAs are reported to act as key regulator in the development of cancer through inhibiting specific genes involved in cellular mechanisms, including drug resistance, proliferation, apoptosis, invasion and metastasis (8,48). Previous studies have also demonstrated that several miRNAs can function as a tumor suppressor in LSCC by suppressing cellular proliferation, invasion, and promoting apoptosis, including miR-203 and miR-370 (3,11). However, the precise molecular mechanisms for aberrant miRNA expression in LSCC require further investigation for a more detailed understanding. In the present study, the miRNA expression profiles in LSCC were investigated and the molecular mechanism underlying the biological function of miRNAs in the development of LSCC were examined. It was found that miR-143-3p was downregulated in LSCC tissues and that the ectopic expression of miR-143-3p predicted poor prognosis in LSCC. The overexpression of miR-143-3p inhibited cellular proliferation and promoted apoptosis *in vitro*, and suppressed tumor growth *in vivo*. In addition, the upregulation of miR-143-3p repressed cell migration and invasion via suppressing EMT and MMP-9. The results demonstrated that miR-143-3p may exert anticancer effects on LSCC via targeting the k-Ras/Raf/MEK/ERK signaling pathway.

Previous studies have reported that miR-143-3p is down-regulated in different types of cancer and functions as a tumor suppressor to control various biological processes, including cell proliferation, apoptosis and migration (12,13). However, the role of miR-143-3p in LSCC remained unclear. In the present

study, microarray analysis showed that the expression levels of several miRNAs were altered in LSCC tissues, with miR-143-3p being downregulated the most compared with normal tissues. Therefore, miR-143-3p was selected in the present study and its function in the development of LSCC was investigated. The results demonstrated that a low expression of miR-143-3p was positively associated with T classification, differentiation, lymph node metastasis and clinical stage in patients with LSCC. Kaplan-Meier survival analysis illustrated that patients with a low expression of miR-143-3p had a lower overall survival rates. These data suggested that the downregulation of miR-143-3p may be key in the development and progression of LSCC. Subsequently, it was demonstrated that the upregulation of miR-143-3p markedly inhibited cell proliferation and induced apoptosis *in vitro*. Furthermore, miR-143-3p-induced apoptosis in LSCC cells modulated the levels of apoptosis-related proteins (cleaved-caspase-3, Bax and Bcl-2). It is reported that Bcl-2 is involved in mitochondria and that a mitochondrial apoptotic pathway may be caspase-3-independent (49,50). Therefore, it was hypothesized that miR-143-3p may promote apoptosis in LSCC cells through regulation of the mitochondrial apoptotic pathway. Additionally, the xenograft model demonstrated that the overexpression of miR-143-3p suppressed tumor growth *in vivo*. Taken together, these results suggested that a low expression of miR-143-3p was significantly associated with poor prognosis in patients with LSCC, and acts as a tumor suppressor in LSCC tumorigenesis.

Cell invasion and migration are known to be key factors in malignant progression and metastasis. A previous study also indicated that recurrence and metastasis are major factors limiting the successful treatment of LSCC (4). To further evaluate the effects of miR-143-3p on tumor cell metastasis, Transwell invasion and wound-healing assays were performed to investigate LSCC cell invasion and migration following the upregulation of miR-143-3p. It was found that the overexpression of miR-143-3p significantly repressed cell migration and invasion *in vitro*. EMT is one of the key molecular steps in the process of distant metastasis, which results in invasion and emigration in different types of cancer (51,52). The EMT cascade can result in loss of apicobasolateral polarity and dissolution of cell-cell junctions, causing the formation of migratory mesenchymal cells with invasive properties (42). A previous study reported that miR-143-3p serves as a tumor suppressor via regulating the EMT pathway in esophageal squamous cell carcinoma (12). Additionally, MMP-9 was shown to be involved in the development of EMT phenotype in LSCC (41), and patients with LSCC with a low expression of MMP-9 had a higher 5-year survival rate (53). Therefore, a western blot assay was performed in the present study to detect the protein expression of EMT markers (E-cadherin, N-cadherin and vimentin) and MMP-9 in LSCC cells following the overexpression of miR-143-3p. The results demonstrated that the upregulation of miR-143-3p increased the protein level of E-cadherin and reduced the levels of N-cadherin, vimentin and MMP-9. Collectively, these data indicated that miR-143-3p repressed cell migration and invasion via inhibiting the EMT cascade and expression of MMP-9 in LSCC cells.

The oncogene k-Ras modulates a multilayered signaling network in various cancer cells, including proliferation, apoptosis, survival, transformation and EMT (21-24,54). k-Ras is considered

to be one of the most prominent oncogenes owing to its ability to transform human cells into malignant tumor cells, with missense mutations at codons 12 or 13 (55). In addition, miR-143-3p has been shown to act as a tumor suppressor via targeting oncogene k-Ras in renal cell carcinoma (44). In the present study, it was confirmed that k-Ras is a direct target of miR-143-3p in LSCC cells. In addition, the expression levels of k-Ras in LSCC tumor tissues were inversely correlated with levels of miR-143-3p. The overexpression of k-Ras abrogated the suppressive effects of miR-143-3p on cell growth, migration and invasion in LSCC cells. These results suggested that miR-143-3p possessed suppressive effects on LSCC cells through targeting k-Ras.

Raf/1 is one of the RAF kinase family members, also termed c-Raf (56). Evidence indicates that Raf/1 is involved in the regulation of endothelial apoptosis and angiogenesis, which is essential in the development and metastasis of tumors (57,58). Raf/1 protein phosphorylates MEK1/2, which can phosphorylate ERK1/2 (56). A previous study documented that k-Ras activated the Raf/MEK/ERK pathway, occurring in ~30% of cancer cases (16). Therefore, to evaluate whether miR-143-3p can regulate the Raf/MEK/ERK pathway in LSCC cells via targeting k-Ras, the present study measured the levels of k-Ras, Raf/1, MEK1/2 and ERK1/2 in LSCC cells transfected with miR-143-3p mimic or NC mimic. The western blot analysis showed that the overexpression of miR-143-3p resulted in the downregulation of p-k-Ras, p-Raf/1, p-MEK1/2 and p-ERK1/2. Furthermore, the results demonstrated that a low expression of miR-143-3p in LSCC tissues was associated with increased expression of p-Raf/1 and p-ERK1/2. Taken together, these data suggested that miR-143-3p may inhibit cell growth, migration and invasion in LSCC through suppressing the k-Ras/Raf/MEK/ERK signaling pathway.

In conclusion, the results of the present study demonstrated that miR-143-3p was downregulated in LSCC tumor tissues, and that the low expression of miR-143-3p predicted poor prognosis in LSCC. The overexpression of miR-143-3p suppressed tumor cell growth and metastasis *in vitro* and *in vivo*. Furthermore, it was found that miR-143-3p possesses suppressive effects on LSCC via inhibiting the k-Ras/Raf/MEK/ERK signaling pathway. The effects of miR-143-3p may be closely associated with the mitochondrial apoptotic pathway and EMT cascade (Fig. 7). Collectively, these findings provide evidence supporting the role of miR-143-3p as a tumor suppressor in LSCC by targeting k-Ras.

Acknowledgements

Not applicable.

Funding

No funding was received.

Availability of data and materials

All data generated or analyzed during the present study are included in the published article.

Authors' contributions

FZ performed the experiments, contributed to data analysis and wrote the manuscript. HC analyzed the data. FZ and HC

conceptualized the study design, contributed to data analysis and experimental materials. All authors read and approved the final manuscript.

Ethics approval and consent to participate

All patients provided written informed consent for the use of the tumor tissues for clinical investigation. The Institute Research Medical Ethics Committee of Zhengzhou University granted approval for the study. All animal procedures were approved by the Animal Care Committee of the Zhengzhou University.

Patient consent for publication

Not applicable.

Competing interests

The authors declare that they have no competing interests.

References

1. Chu EA and Kim YJ: Laryngeal cancer: diagnosis and preoperative work-up. *Otolaryngol Clin North Am* 41: 673-695, 2008.
2. Tian Y, Fu S, Qiu GB, Xu ZM, Liu N, Zhang XW, Chen S, Wang Y, Sun KL and Fu WN: MicroRNA-27a promotes proliferation and suppresses apoptosis by targeting PLK2 in laryngeal carcinoma. *BMC Cancer* 14: 678, 2014.
3. Ren J, Zhu D, Liu M, Sun Y and Tian L: Downregulation of miR-21 modulates Ras expression to promote apoptosis and suppress invasion of Laryngeal squamous cell carcinoma. *Eur J Cancer* 46: 3409-3416, 2010.
4. Rudolph E, Dyckhoff G, Becher H, Dietz A and Ramroth H: Effects of tumour stage, comorbidity and therapy on survival of laryngeal cancer patients: A systematic review and a meta-analysis. *Eur Arch Otorhinolaryngol* 268: 165-179, 2011.
5. Croce CM: Causes and consequences of microRNA dysregulation in cancer. *Nat Rev Genet* 10: 704-714, 2009.
6. Bartel DP: MicroRNAs: Target recognition and regulatory functions. *Cell* 136: 215-233, 2009.
7. Zhuang LK, Xu GP, Pan XR, Lou YJ, Zou QP, Xia D, Yan WW, Zhang YT, Jia PM and Tong JH: MicroRNA-181a-mediated downregulation of AC9 protein decreases intracellular cAMP level and inhibits ATRA-induced APL cell differentiation. *Cell Death Dis* 5: e1161, 2014.
8. Zhang B, Pan X, Cobb GP and Anderson TA: microRNAs as oncogenes and tumor suppressors. *Dev Biol* 302: 1-12, 2007.
9. Shen Z, Zhan G, Ye D, Ren Y, Cheng L, Wu Z and Guo J: MicroRNA-34a affects the occurrence of laryngeal squamous cell carcinoma by targeting the antiapoptotic gene survivin. *Med Oncol* 29: 2473-2480, 2012.
10. Tian L, Li M, Ge J, Guo Y, Sun Y, Liu M and Xiao H: miR-203 is downregulated in laryngeal squamous cell carcinoma and can suppress proliferation and induce apoptosis of tumours. *Tumour Biol* 35: 5953-5963, 2014.
11. Yungang W, Xiaoyu L, Pang T, Wenming L and Pan X: miR-370 targeted FoxM1 functions as a tumor suppressor in laryngeal squamous cell carcinoma (LSCC). *Biomed Pharmacother* 68: 149-154, 2014.
12. He Z, Yi J, Liu X, Chen J, Han S, Jin L, Chen L and Song H: miR-143-3p functions as a tumor suppressor by regulating cell proliferation, invasion and epithelial-mesenchymal transition by targeting QKI-5 in esophageal squamous cell carcinoma. *Mol Cancer* 15: 51, 2016.
13. Li D, Hu J, Song H, Xu H, Wu C, Zhao B, Xie D, Wu T, Zhao J and Fang L: miR-143-3p targeting LIM domain kinase 1 suppresses the progression of triple-negative breast cancer cells. *Am J Transl Res* 9: 2276-2285, 2017.
14. Campbell SL, Khosravi-Far R, Rossman KL, Clark GJ and Der CJ: Increasing complexity of Ras signaling. *Oncogene* 17 (11 Reviews): 1395-1413, 1998.
15. Vojtek AB and Der CJ: Increasing complexity of the Ras signaling pathway. *J Biol Chem* 273: 19925-19928, 1998.

16. Campbell PM, Groehler AL, Lee KM, Ouellette MM, Khazak V and Der CJ: K-Ras promotes growth transformation and invasion of immortalized human pancreatic cells by Raf and phosphatidylinositol 3-kinase signaling. *Cancer Res* 67: 2098-2106, 2007.
17. Kim MJ, Woo SJ, Yoon CH, Lee JS, An S, Choi YH, Hwang SG, Yoon G and Lee SJ: Involvement of autophagy in oncogenic K-Ras-induced malignant cell transformation. *J Biol Chem* 286: 12924-12932, 2011.
18. Voice JK, Klemke RL, Le A and Jackson JH: Four human ras homologs differ in their abilities to activate Raf-1, induce transformation, and stimulate cell motility. *J Biol Chem* 274: 17164-17170, 1999.
19. Maehara Y, Saeki H and Morita M: Molecular mechanisms of esophageal squamous cell carcinogenesis: Clues to improve treatment outcomes. *Ann Thorac Cardiovasc Surg* 16: 387-388, 2010.
20. Keohavong P, Mady HH, Gao WM, Siegfried JM, Luketich JD and Melhem MF: Topographic analysis of K- ras mutations in histologically normal lung tissues and tumours of lung cancer patients. *Br J Cancer* 85: 235-241, 2001.
21. Karnoub AE and Weinberg RA: Ras oncogenes: Split personalities. *Nat Rev Mol Cell Biol* 9: 517-531, 2008.
22. Pylayeva-Gupta Y, Grabocka E and Bar-Sagi D: RAS oncogenes: Weaving a tumorigenic web. *Nat Rev Cancer* 11: 761-774, 2011.
23. Samatar AA and Poulidakos PI: Targeting RAS-ERK signalling in cancer: Promises and challenges. *Nat Rev Drug Discov* 13: 928-942, 2014.
24. Cox AD, Fesik SW, Kimmelman AC, Luo J and Der CJ: Drugging the undruggable RAS: Mission possible? *Nat Rev Drug Discov* 13: 828-851, 2014.
25. Hatley ME, Patrick DM, Garcia MR, Richardson JA, Bassel-Duby R, van Rooij E and Olson EN: Modulation of K-Ras-dependent lung tumorigenesis by MicroRNA-21. *Cancer Cell* 18: 282-293, 2010.
26. Zhou K, Luo X, Wang Y, Cao D and Sun G: MicroRNA-30a suppresses tumor progression by blocking Ras/Raf/MEK/ERK signaling pathway in hepatocellular carcinoma. *Biomed Pharmacother* 93: 1025-1032, 2017.
27. Zhou L, Rui JA, Ye DX, Wang SB, Chen SG and Qu Q: Edmondson-Steiner grading increases the predictive efficiency of TNM staging for long-term survival of patients with hepatocellular carcinoma after curative resection. *World J Surg* 32: 1748-1756, 2008.
28. Ma J, Ren Y, Zhang L, Kong X, Wang T, Shi Y and Bu R: Knocking-down of CREPT prohibits the progression of oral squamous cell carcinoma and suppresses cyclin D1 and c-Myc expression. *PLoS One* 12: e0174309, 2017.
29. Livak KJ and Schmittgen TD: Analysis of relative gene expression data using real-time quantitative PCR and the 2(-Δ ΔC(T)) Method. *Methods* 25: 402-408, 2001.
30. Lai YJ, Lin CI, Wang CL and Chao JI: Expression of survivin and p53 modulates honokiol-induced apoptosis in colorectal cancer cells. *J Cell Biochem* 115: 1888-1899, 2014.
31. Schipper JH, Frixen UH, Behrens J, Unger A, Jahnke K and Birchmeier W: E-cadherin expression in squamous cell carcinomas of head and neck: Inverse correlation with tumor dedifferentiation and lymph node metastasis. *Cancer Res* 51: 6328-6337, 1991.
32. Gotoda T, Yanagisawa A, Sasako M, Ono H, Nakanishi Y, Shimoda T and Kato Y: Incidence of lymph node metastasis from early gastric cancer: Estimation with a large number of cases at two large centers. *Gastric Cancer* 3: 219-225, 2000.
33. Hartgrink HH, van de Velde CJ, Putter H, Bonenkamp JJ, Klein Kranenbarg E, Songun I, Welvaart K, van Krieken JH, Meijer S, Plukker JT, *et al*: Extended lymph node dissection for gastric cancer: Who may benefit? Final results of the randomized Dutch gastric cancer group trial. *J Clin Oncol* 22: 2069-2077, 2004.
34. Bergers G, Brekken R, McMahon G, Vu TH, Itoh T, Tamaki K, Tanzawa K, Thorpe P, Itohara S, Werb Z, *et al*: Matrix metalloproteinase-9 triggers the angiogenic switch during carcinogenesis. *Nat Cell Biol* 2: 737-744, 2000.
35. Kang Y and Massagué J: Epithelial-mesenchymal transitions: Twist in development and metastasis. *Cell* 118: 277-279, 2004.
36. Natalwala A, Spychal R and Tselepis C: Epithelial-mesenchymal transition mediated tumorigenesis in the gastrointestinal tract. *World J Gastroenterol* 14: 3792-3797, 2008.
37. Eriksen JG, Steiniche T, Sogaard H and Overgaard J: Expression of integrins and E-cadherin in squamous cell carcinomas of the head and neck. *APMIS* 112: 560-568, 2004.
38. Zhang SY, Lu ZM, Lin YF, Chen LS, Luo XN, Song XH, Chen SH and Wu YL: miR-144-3p, a tumor suppressive microRNA targeting ETS-1 in laryngeal squamous cell carcinoma. *Oncotarget* 7: 11637-11650, 2016.
39. Schmalhofer O, Brabletz S and Brabletz T: E-cadherin, beta-catenin, and ZEB1 in malignant progression of cancer. *Cancer Metastasis Rev* 28: 151-166, 2009.
40. Li JZ, Gao W, Lei WB, Zhao J, Chan JY, Wei WI, Ho WK and Wong TS: MicroRNA 744-3p promotes MMP-9-mediated metastasis by simultaneously suppressing PDCD4 and PTEN in laryngeal squamous cell carcinoma. *Oncotarget* 7: 58218-58233, 2016.
41. Zhang W, Liu Y and Wang CW: S100A4 promotes squamous cell laryngeal cancer Hep-2 cell invasion via NF-κB/MMP-9 signal. *Eur Rev Med Pharmacol Sci* 18: 1361-1367, 2014.
42. Hur K, Toiyama Y, Takahashi M, Balaguer F, Nagasaka T, Koike J, Hemmi H, Koi M, Boland CR and Goel A: MicroRNA-200c modulates epithelial-to-mesenchymal transition (EMT) in human colorectal cancer metastasis. *Gut* 62: 1315-1326, 2013.
43. Han Z, Yang Q, Liu B, Wu J, Li Y, Yang C and Jiang Y: MicroRNA-622 functions as a tumor suppressor by targeting K-Ras and enhancing the anticarcinogenic effect of resveratrol. *Carcinogenesis* 33: 131-139, 2012.
44. Zhai W, Sun Y, Guo C, Hu G, Wang M, Zheng J, Lin W, Huang Q, Li G, Zheng J, *et al*: lncRNA-SARCC suppresses renal cell carcinoma (RCC) progression via altering the androgen receptor(AR)/miRNA-143-3p signals. *Cell Death Differ* 24: 1502-1517, 2017.
45. Ramos JW: The regulation of extracellular signal-regulated kinase (ERK) in mammalian cells. *Int J Biochem Cell Biol* 40: 2707-2719, 2008.
46. McCubrey JA, Steelman LS, Chappell WH, Abrams SL, Wong EW, Chang F, Lehmann B, Terrian DM, Milella M, Tafuri A, *et al*: Roles of the Raf/MEK/ERK pathway in cell growth, malignant transformation and drug resistance. *Biochim Biophys Acta* 1773: 1263-1284, 2007.
47. Zhang X, Mao H, Chen JY, Wen S, Li D, Ye M and Lv Z: Increased expression of microRNA-221 inhibits PAK1 in endothelial progenitor cells and impairs its function via c-Raf/MEK/ERK pathway. *Biochem Biophys Res Commun* 431: 404-408, 2013.
48. Coburn GA and Cullen BR: siRNAs: A new wave of RNA-based therapeutics. *J Antimicrob Chemother* 51: 753-756, 2003.
49. Cheng EH, Wei MC, Weiler S, Flavell RA, Mak TW, Lindsten T and Korsmeyer SJ: BCL-2, BCL-X(L) sequester BH3 domain-only molecules preventing BAX- and BAK-mediated mitochondrial apoptosis. *Mol Cell* 8: 705-711, 2001.
50. Ochs K and Kaina B: Apoptosis induced by DNA damage O6-methylguanine is Bcl-2 and caspase-9/3 regulated and Fas/caspase-8 independent. *Cancer Res* 60: 5815-5824, 2000.
51. Yang J and Weinberg RA: Epithelial-mesenchymal transition: At the crossroads of development and tumor metastasis. *Dev Cell* 14: 818-829, 2008.
52. Jou J and Diehl AM: Epithelial-mesenchymal transitions and hepatocarcinogenesis. *J Clin Invest* 120: 1031-1034, 2010.
53. Gou X, Chen H, Jin F, Wu W, Li Y, Long J, Gong X, Luo M, Bi T, Li Z, *et al*: Expressions of CD147, MMP-2 and MMP-9 in laryngeal carcinoma and its correlation with poor prognosis. *Pathol Oncol Res* 20: 475-481, 2014.
54. Malumbres M and Barbacid M: RAS oncogenes: The first 30 years. *Nat Rev Cancer* 3: 459-465, 2003.
55. Shimizu K, Goldfarb M, Suard Y, Perucho M, Li Y, Kamata T, Feramisco J, Stavnezer E, Fogh J and Wigler MH: Three human transforming genes are related to the viral ras oncogenes. *Proc Natl Acad Sci USA* 80: 2112-2116, 1983.
56. Davies H, Bignell GR, Cox C, Stephens P, Edkins S, Clegg S, Teague J, Woffendin H, Garnett MJ, Bottomley W, *et al*: Mutations of the BRAF gene in human cancer. *Nature* 417: 949-954, 2002.
57. Alavi A, Hood JD, Frausto R, Stupack DG and Cheresch DA: Role of Raf in vascular protection from distinct apoptotic stimuli. *Science* 301: 94-96, 2003.
58. Hood JD, Bednarski M, Frausto R, Guccione S, Reisfeld RA, Xiang R and Cheresch DA: Tumor regression by targeted gene delivery to the neovasculature. *Science* 296: 2404-2407, 2002.